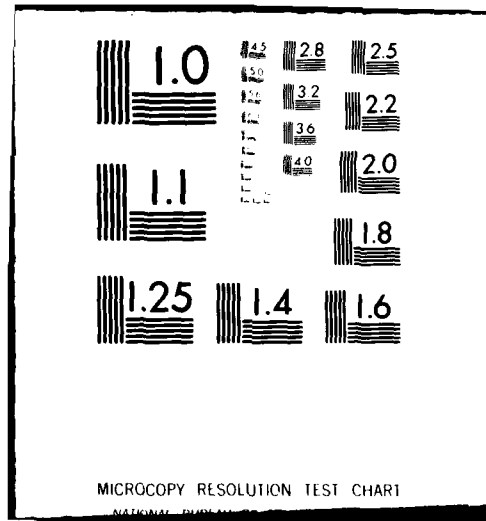AD-A094 194   MASSACHUSETTS INST OF TECH CAMBRIDGE CENTER FOR MATE--ETC F/G 14/2
                MICRODIELECTROMETRY: A NEW METHOD FOR IN SITU CURE MONITORING.(U)
                DEC 80 N F SHEPPARD, S L GARVERICK, D R DAY   N00014-78-C-0591
UNCLASSIFIED   NL

END
DATE
FILMED
2 -81
DTIC

1.0

1.1

1.25 1.4 1.6

45 2.8 2.5
50 3.2 2.2
36
40 2.0

1.8

MICROCOPY RESOLUTION TEST CHART

LEVEL

⑫

OFFICE OF NAVAL RESEARCH

Contract N00014-78-C-0591

Task No. NR 356-691

TECHNICAL REPORT NO. 2

Microdielectrometry: A New Method for
In Situ Cure Monitoring

by

Norman F. Sheppard, Steven L. Garverick,
David R. Day and Stephen D. Senturia

Prepared for the Proceedings of the

26th National SAMPE Symposium

MASSACHUSETTS INSTITUTE OF TECHNOLOGY
Department of Electrical Engineering and Computer Science
and Center for Materials Science and Engineering
Cambridge, Massachusetts

December 19, 1980

81 1 26 048

REPORT DOCUMENTATION PAGE		READ INSTRUCTIONS BEFORE COMPLETING FORM
1. REPORT NUMBER	2. GOVT ACCESSION NO. AD-A094	3. RECIPIENT'S CATALOG NUMBER 194
4. TITLE (and Subtitle) MICRODIELECTROMETRY: A NEW METHOD FOR IN SITU CURE MONITORING.		5. TYPE OF REPORT & PERIOD COVERED Technical Report 9/79 - 12/80
		6. PERFORMING ORG. REPORT NUMBER Technical Report No. 2
7. AUTHOR(s) Norman F. Sheppard, Steven L. Garverick, David R. Day and Stephen D. Senturia		8. CONTRACT OR GRANT NUMBER(s) ⑮ N00014-78-C-0591 ✓ NSF-DMR78-24185
9. PERFORMING ORGANIZATION NAME AND ADDRESS Massachusetts Institute of Technology Department of Electrical Engineering and Computer Science, Cambridge, Mass. 02139		10. PROGRAM ELEMENT, PROJECT, TASK, AREA & WORK UNIT NUMBERS NR 356-691
11. CONTROLLING OFFICE NAME AND ADDRESS Department of the Navy, Office of Naval Research 800 N. Quincy Street, Arlington VA 22217 CODE 427		12. REPORT DATE ⑪ 19 December 1980
		13. NUMBER OF PAGES 17
14. MONITORING AGENCY NAME & ADDRESS(if different from Controlling Office) ⑫ 9,21		15. SECURITY CLASS. (of this report) UNCLASSIFIED
		15a. DECLASSIFICATION/DOWNGRADING SCHEDULE

16. DISTRIBUTION STATEMENT (of this Report)

This document has been approved for public release and sale; its distribution is unlimited.

17. DISTRIBUTION STATEMENT (of the abstract entered in Block 20, if different from Report)

18. SUPPLEMENTARY NOTES

19. KEY WORDS (Continue on reverse side if necessary and identify by block number)

Dielectrometry, cure monitoring, epoxy, integrated circuit, charge-flow transistor

20. ABSTRACT (Continue on reverse side if necessary and identify by block number)

Integrated circuit technology has been used to develop a miniature dielectric cure monitor probe that combines small size with built-in amplification for operation down to 1 Hz. This report describes the design and operation of the microdielectrometer chip, and the model used to determine the complex dielectric constant of the material under study. Two typical applications are illustrated by experiments. Postcure data for a Versamide 140, Epon 828 mixture are compared with results from conventional parallel plate dielectrometers, and multi-probe monitoring of cure within a bulk sample of the same resin is examined

MICRODIELECTROMETRY: A NEW METHOD FOR
IN SITU CURE MONITORING

Norman F. Sheppard, Steven L. Garverick, David R. Day,
and Stephen D. Senturia
Department of Electrical Engineering and Computer Science,
and Center for Materials Science and Engineering
Massachusetts Institute of Technology
Cambridge, Massachusetts

ABSTRACT

Integrated circuit technology has been used to develop a miniature dielectric cure monitor probe that combines small size with built in amplification to achieve good sensitivity down to 1 Hz, making the probe more sensitive to physical property changes than conventional dielectrometers operating at 1000 Hz. This paper describes the design and operation of the microdielectrometer chip, and the model used to determine the complex dielectric constant of the material under study. Two typical applications are illustrated by experiments. First, results of a postcure study of a Versamide 140, Epon 828 mixture are presented and compared to the results of a similar study using a conventional parallel plate capacitor. In a second experiment, several probes were placed in a 100 ml mold and used to monitor the cure of a sample of the same resin system. The data show the nonuniformity of cure within the sample, and can be explained on the basis of gelation and the temperature dependence of the dielectric properties as determined in the post-cure experiment.

1. INTRODUCTION

As a result of the widespread use of a large variety of reactive ther-
mosetting resins, a need exists for the ability to study the chemical and
mechanical thermoset properties both as a function of cure and after cure.
Conventional means of analysis for degree of conversion include reactive
group analysis, FTIR, and DSC, while bulk properties can be monitored through
torsional braid analysis, viscosity, and dielectrometry. All of these methods
can be cumbersome, and this has inspired the development of a simple cure
monitoring integrated circuit.

The new microdielectrometer 'chip' measures the low frequency dielec-
tric properties of a resin both during and after cure, as in conventional
dielectric techniques. The integrated sensors present an advantage in that
they are small and can be placed in various locations of a large test sample,
or can serve as implants for long-term property monitoring. The small mass
enables quick thermal equilibration for isothermal or ramped measurements on
small resin samples. The microdielectrometer chip also has the capability of
monitoring much lower frequencies than conventional dielectrometry (down to 1
Hz or below, as opposed to 100 Hz). At these lower frequencies the dielectric
response is more representative of the mechanical properties and therefore
presents a viable alternative to torsional braid analysis. In addition, 'on
chip' signal amplification eliminates the need for electrical shielding and
increases sensitivity.

In this paper we will discuss the device structure and explain its
operation. Initial results will be presented for a thermal ramp of a cured
thermoset and compared to the equivalent results from a conventional parallel
plate arrangement. Also to be presented are the data from a large sample

during cure containing multiple chip sensors at various locations within the bulk. These results will be explained on the basis of gelation and post cure properties as a function of temperature.

2. DEVICE DESIGN

The present microdielectrometer chip evolved from the charge-flow transistor (CFT).[1] A charge-flow transistor consists of a field effect transistor (FET) with a gap in the gate over the critical channel region of the transistor which is filled by the material to be studied. The turn on characteristics of the transistor are determined by the flow of charges from the gate electrode through the material of interest to the channel region. The step waveform response of the CFT has been shown to change as a function of thermoset resin cure and can be explained through suitable modeling of the resin.[2]

The original CFT design was difficult to calibrate, and yielded an output that required nonlinear large signal analysis for interpretation. For this reason, a new sensor has been developed which can be analyzed with linear device models, and which permits accurately calibrated measurements to be made using differential techniques.[3] In this design, the device response is balanced against a reference FET so that all device characteristics are cancelled, leaving only the desired response of the material under study.

The new chip is 75 mils square, and employs a large area interdigitated capacitor as the sensing element. A sinusoidal voltage applied to one electrode, the "driven electrode" (see Fig. 1), transfers charge through the material under study to the opposite electrode, "the sensing electrode". As with standard parallel plate capacitors, the current due to this charge
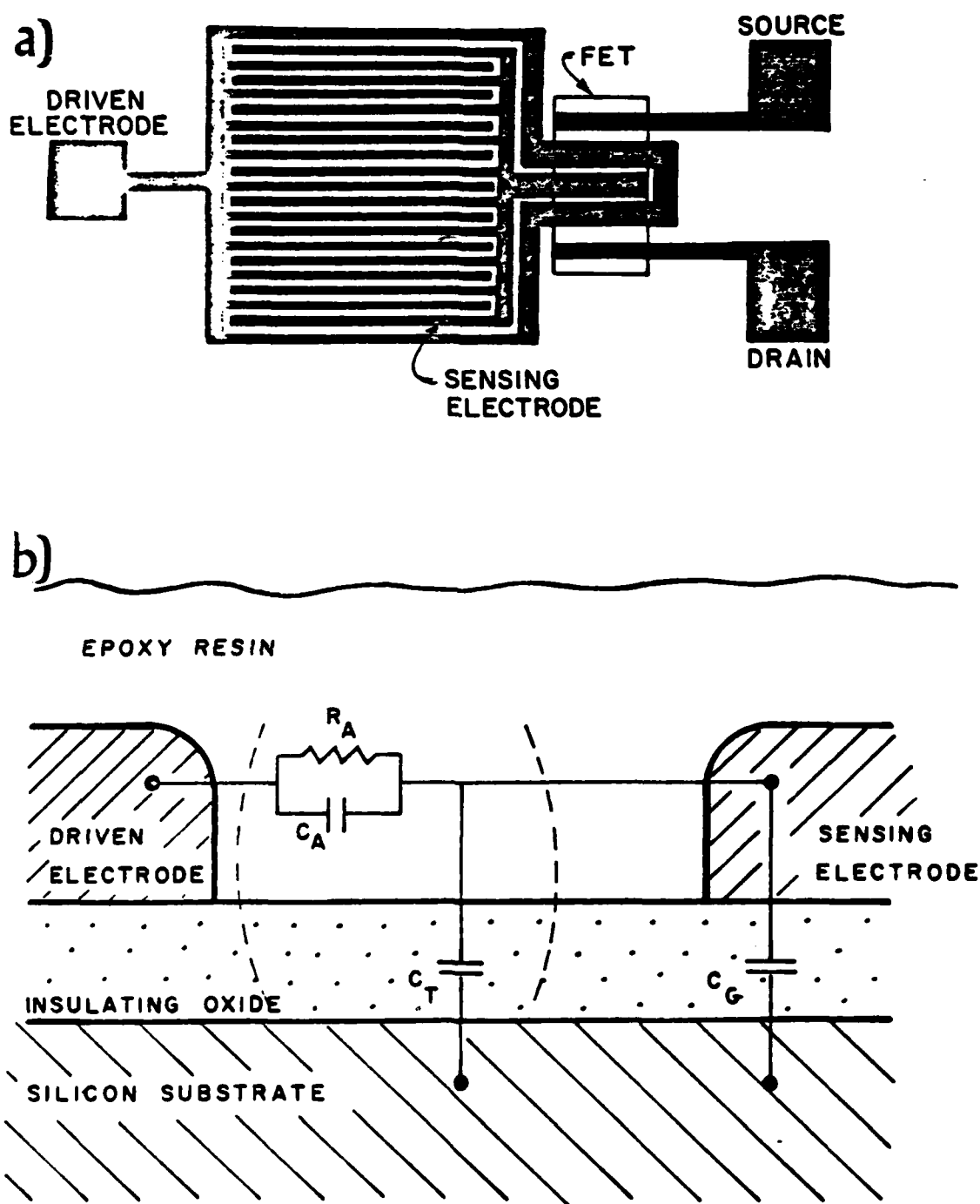
Fig.1 a) Schematic top view of the active portion of the microdielectrometer chip. b) Schematic cross-section of the transfer function model.

transfer could be measured with a capacitance bridge or dielectrometer using shielded cables and other appropriate measures to prevent noise. Noise problems are largely eliminated in the new chip by attaching the low side of the interdigitated capacitor (the sensing electrode) directly to the gate of a depletion-mode FET operating in its linear region. The presence of charge on this gate produces a voltage that controls the current flowing between the drain and source terminals of the transistor. The drain to source current resulting from a sinusoidal driving voltage contains the same information about charge transfer through the material as the conventional capacitor current, but is about 10^6 times larger. This on-chip amplification enables measurement of dielectric properties down to 1 Hz, a frequency at which capacitor currents are too small to be measured in a conventional manner.

3. MEASUREMENT CIRCUIT

The function of the measurement circuit (which is described in detail in Reference 3) is to measure the drain to source current of the sensing FET, and from it, to infer the sensing gate voltage which is directly related to the charge transfer from the driven gate to the sensing gate. To do this, a second depletion mode FET, identical in all dimensions to the sensing FET, is included on the chip as a reference. The gate of the reference FET is driven by an off chip current comparator so that the currents in both FETs are equal. Since the device geometries are identical, the voltage applied by the current comparator to the reference FET is necessarily equal to the voltage on the floating gate of the sensing FET. This measurement technique provides an output voltage equal to that on the floating gate and eliminates any current offset due to temperature variations, enabling the chip to function at temperatures up to 250°C.

During an experiment, the driven gate voltage and the reference voltage are simultaneously sent to a HP3575A gain-phase meter which determines the ratio of their amplitudes and relative phase shift. The digitized information is logged in real time by a HP85 desktop computer. The HP85 also controls a HP3325A function generator, which sets the frequency and amplitude of the driven gate voltage. This system allows for real time measurement as a function of frequency, temperature, and cure. The system is also capable of taking measurements on multiple devices through automatic switching, enabling cure data to be obtained from various regions within a sample simultaneously.

4. TRANSFER FUNCTION MODEL

The transfer function for the planar interdigitated capacitor is somewhat more complicated than that for a conventional parallel plate geometry. The dependence of the amplitude and phase of the sensing gate voltage on the complex dielectric constant of the resin (permittivity ϵ', and loss factor ϵ'') can be modeled by a one-dimensional distributed RC circuit, as illustrated in Fig. 1. The bracketed elements represent a differential element of the distributed system. C_A is proportional to ϵ', and R_A is proportional to $1/\omega\epsilon''$, where ω is the angular frequency. Thus, $\tan\delta = 1/\omega R_A C_A$. C_T represents the capacitance between the plane of the electrode and the ground plane beneath the silicon dioxide, and C_G represents the total gate capacitance of the sensing FET and sensing electrode.

The exact transfer function for this model is given in the Appendix. The calibration of the device depends on C_T, C_G, and the separation betweeen electrodes, all of which can be controlled by device design and processing

conditions. With this information, plus a single semi-empirical thickness parameter, d, there is a unique relation of ε' and ε'' to the magnitude and phase of the sensing gate voltage relative to the driven gate voltage.

5. EXPERIMENTAL

Initial experimentation has been carried out on an equal volume mix of Versamide 140, a linear aliphatic amide, and EPON 828 (DGEBA). This system was chosen because of its reasonably short cure time in 100ml batches at room temperature and the realitively low glass-rubber transition in the post cured material.

Two types of experiments were performed. For the study of fully cured material, samples were prepared by placing small drops of the resin on the chip sensing area and then curing at 180°C for 10 minutes. A parallel plate capacitor was also filled with the resin and cured under the same conditions. After cure, dielectric measurements were monitored at three frequencies (10, 100, and 1000 Hz) during a temperature ramp from 60°C at 4 deg/min.

In a second experiment to demonstrate the cure monitoring ability, several chips were placed at various levels within an empty mold (5.5 x 5.5 cm). An integrated temperature sensor (Analog Devices AD590) was included alongside each sensing chip for accurate temperature tracking during the cure. After the epoxy was mixed and poured into the mold, automatic measurements were initiated. The dielectric response and temperature were monitored during cure as a function of three frequencies (10, 100, and 1000 Hz).

6.0 RESULTS

6.1 Fully Cured Material

The dielectric behavior of the cured material as measured in the parallel plate capacitor is indicated in Fig. 2. The ε' data exhibit a frequency dependent transition which we attribute to dipole relaxation associated with the glass-rubber transition.[4] The ε'' behavior exhibits a steeply rising term on which are superimposed small peaks that one expects from the dipole relaxation. This suggests the existence of an activated ohmic conductivity of the following form:[4]

$$\sigma(T) = \sigma_o \exp(-E_C/kT) \tag{1}$$

where $\sigma(T)$ is the conductivity and E_C is the activation energy. The conductivity observed in the parallel plate data, which is most likely due to ionic conduction, is found to have an activation energy of 6.5 kcal/mole.

The relative amplitude (gain in decibels) and phase response of the microdielectrometer for fully cured material as a function of temperature is shown in Fig. 3. Using the relations in the Appendix, ε' and ε'' values were obtained from these data, and are shown in Fig. 4. The ε' values show excellent agreement with the parallel plate data, but there is a significant difference in the ε'' values. The conductance peaks correspond closely to those expected from normal dipole relaxation, but the strong ionic conductance observed in the parallel plate experiment appears to be missing. As a test, a conduction term of the form of Eq. 1 was added to the microdielectrometer data, resulting in the graphs of Fig. 5, which correspond quite closely with the parallel plate results of Fig. 3. Thus it appears that the planar electrode technique is sensitive only to dielectric loss contributions
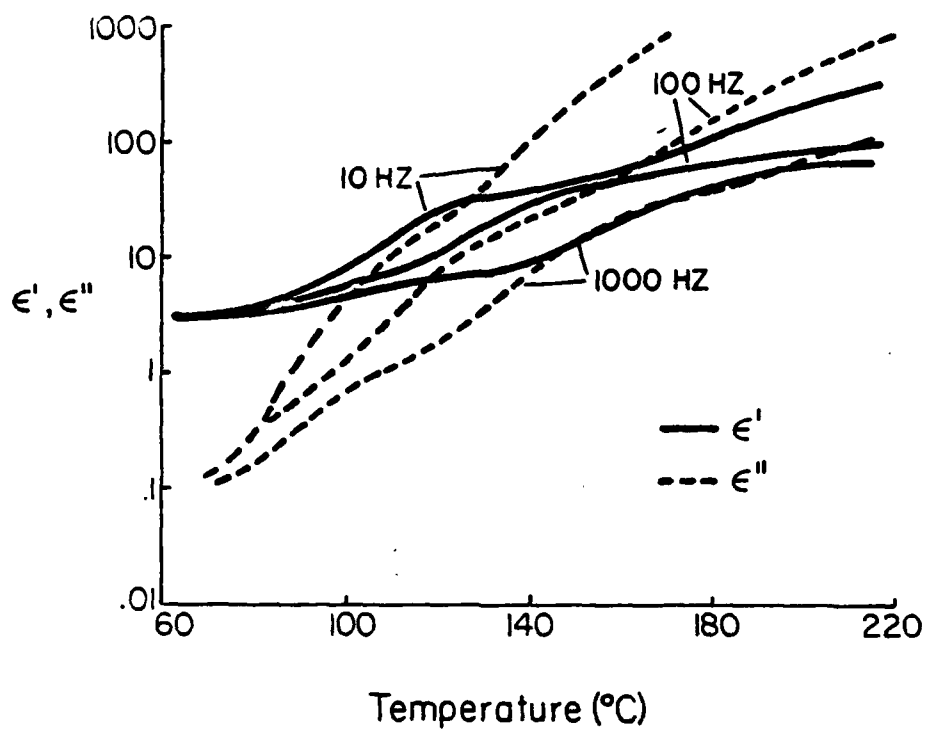
Fig. 2 Dielectric spectra of fully cured epoxy from parallel plate capacitor measurement.
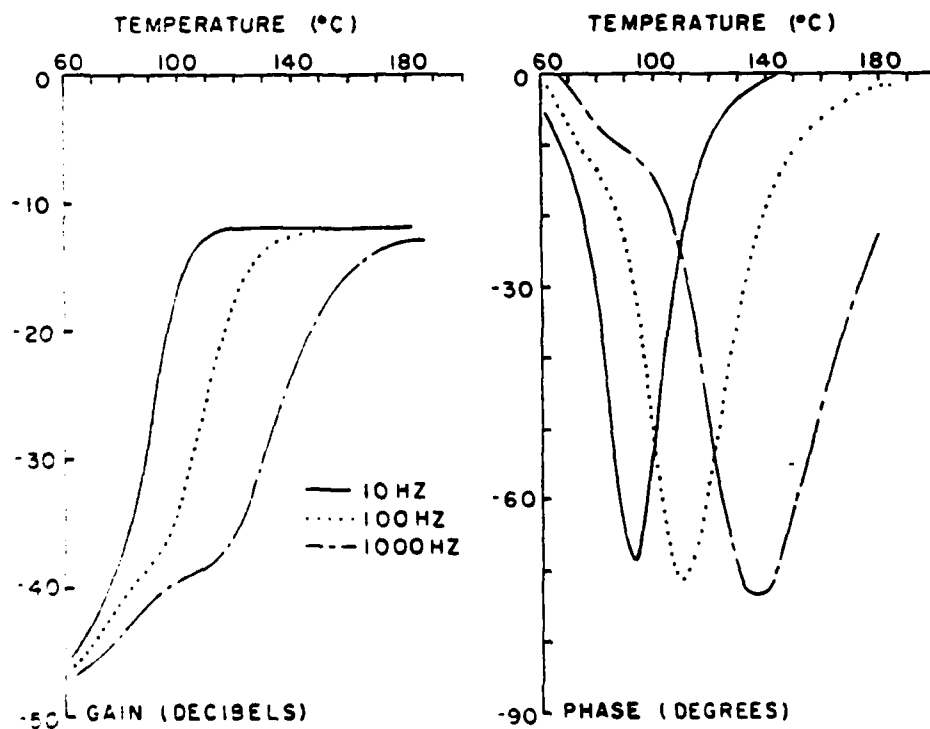

Fig. 3 Raw data (gain and phase) for fully cured epoxy as a function of temperature from the microdielectrometer chip.
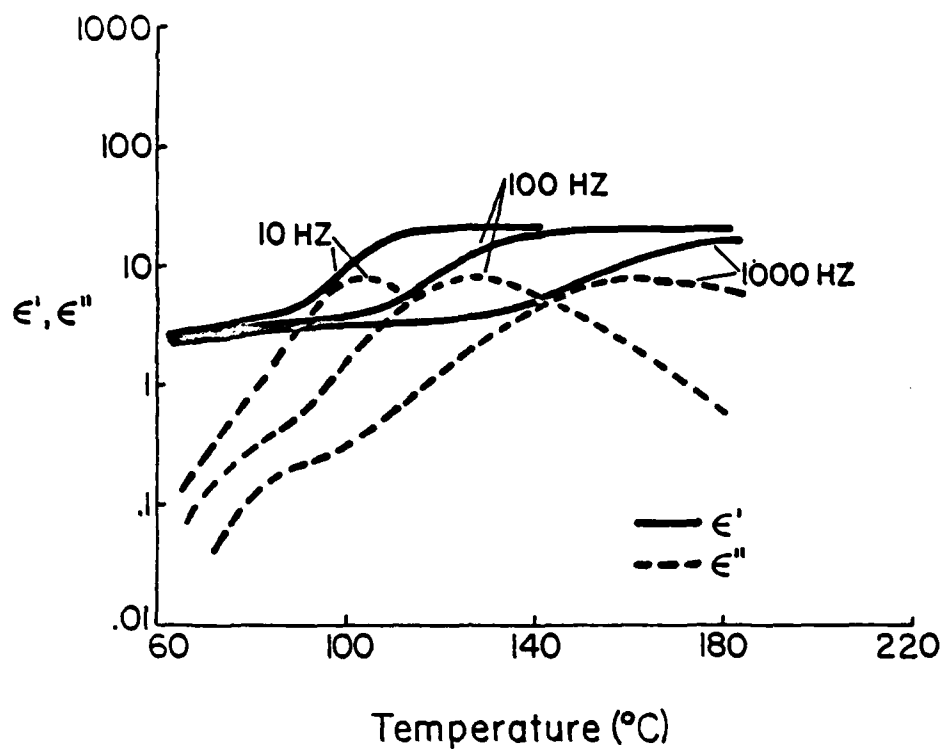
Fig. 4 Dielectric spectra of fully cured epoxy calculated from the data of Fig. 3 using the transfer function in the Appendix.
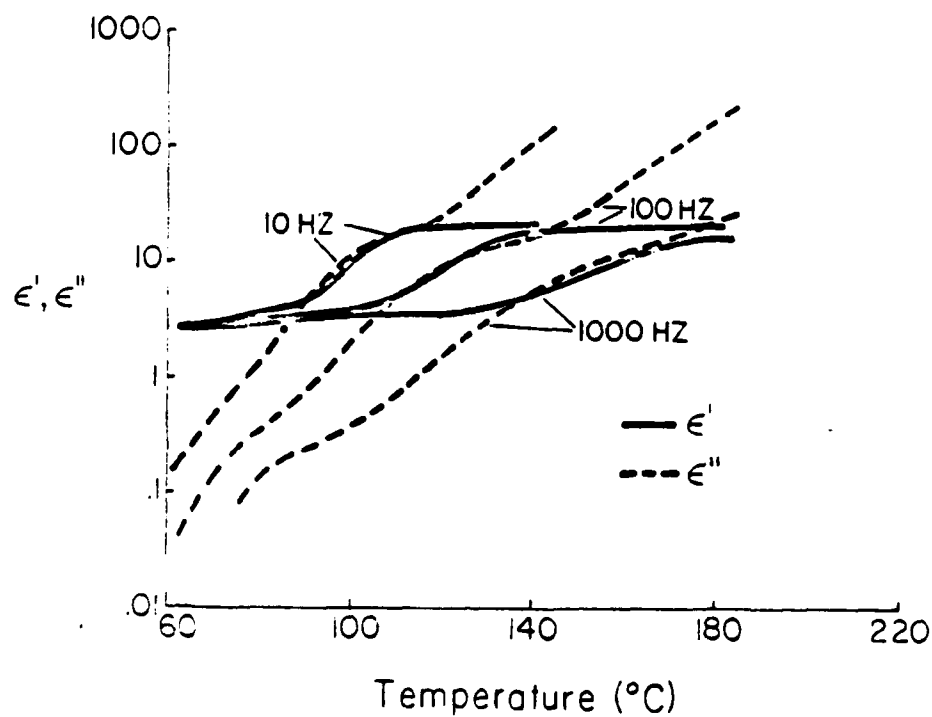

Fig. 5 Dielectric spectra of fully cured epoxy calculated from Fig. 4 with the addition of an ohmic conductivity (Eq. 1).

from dipole relaxation and is immune to ohmic conductivity, at least for this material and under these conditions. This behavior is presently not understood, but may be of great benefit in observing relaxation phenomena that are normally obscured by high ohmic conductivities.

6.2 Multiple Chip Cure Monitoring

During the cure of the large epoxy sample containing multiple sensors, the exothermic reaction caused the temperature to rise from 20°C to 130°C just after gelation and then finally settle back down to 20°C. As a result of the positioning of the sensors in the mold, different temperature profiles and dielectric responses were observed.

Raw data from the devices at the bottom and center of the mold are shown in Fig. 6. The temperature profiles indicate a slightly faster rise in temperature in the center of the mold than at the bottom, as expected.

The sharp discontinuity in the gain and phase data near 100 minutes is attributed to the gel point, for two reasons. First, the slope of the temperature profile starts decreasing at this point, and within a few minutes, the actual temperature starts to decrease, indicating a sharp reduction in reaction rate. Crosslinking reactions are known to be inhibited after gelation as a result of the formation of an infinite network which greatly impedes the diffusion of reactants to reaction sites. Second, the behavior of the gain and phase after the occurance of the sharp discontinuity are nearly identical to that of the fully cured material shown in Fig. 2. Using the phase versus temperature data of the fully cured material, the phase has been replotted as a function of the temperature profile from Fig. 6. In the resulting curves (Fig. 7), the phase matches very closely to that observed in
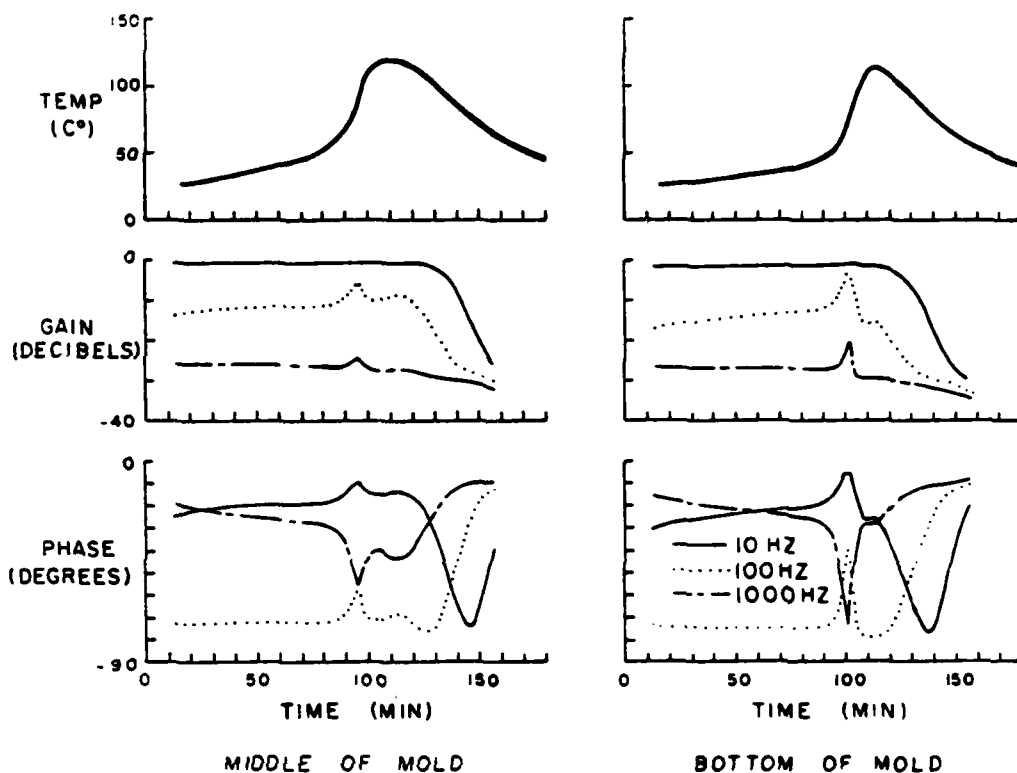
Fig. 6 Gain and phase response of microdielectrometer chips located in the
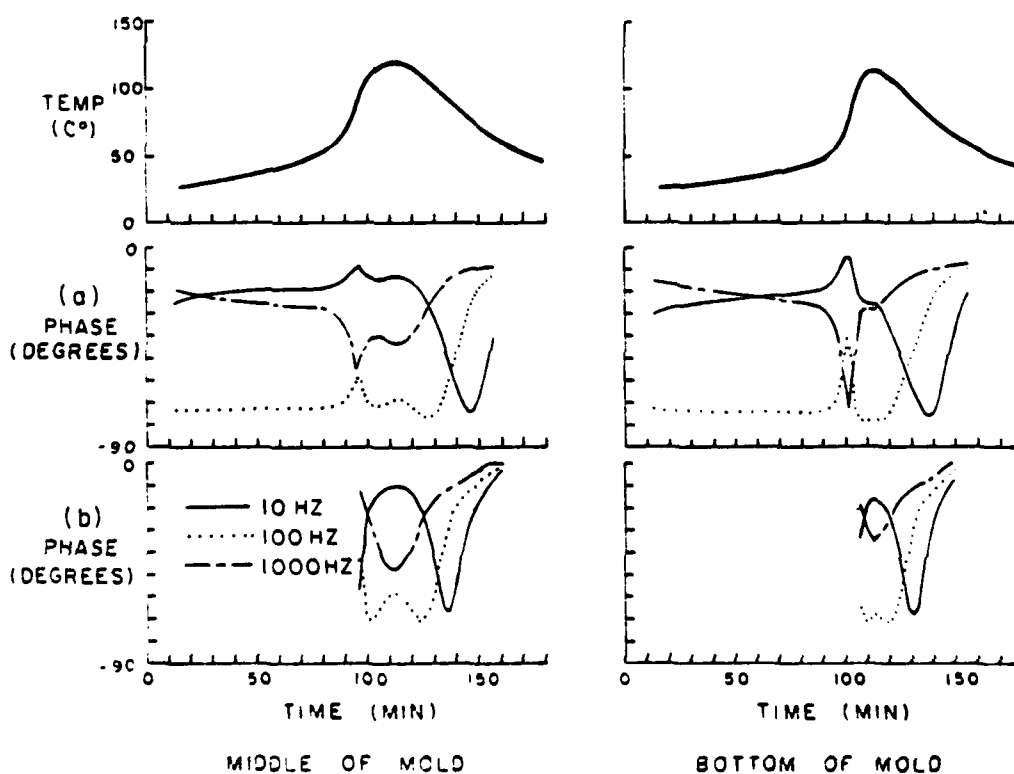bottom and center of a 5.5x5.5 cm cylindrical mold during epoxy cure.

Fig. 7 Comparison of a) measured phase response of microdielectrometer
during epoxy cure to b) the corresponding phase response measured for the
fully cured material at equivalent temperatures.

the mold cure at times beyond the gelation point. This similarity in behavior indicates that the peaks that occur after gelation are a result of the temperature passing above and then back down through the relaxation temperature of the cured material.

As a result of the sharp discontinuity in gain and phase at gelation, differences in gel point times for the various sensor locations are easily determined. In this particular sample the middle of the resin gelled five minutes before the bottom, which was only two centimeters away. This result stresses the difference in reaction rates which can occur from variation in mold geometry and temperature.

7. DISCUSSION

The microdielectrometer chip has been shown to yield results in general agreement with the results of conventional parallel plate dielectrometry. Advantages of the chip lie in its small size, making implantation and measurements on small samples possible. On-chip amplification also eliminates the need for electrical shielding. In addition, the chip has frequency monitoring ability down to 1 Hz. Low frequency monitoring is useful for observing long relaxation times which occur far into cure and which are generally difficult to measure.

Further improvements in the chip are planned, including the addition of the current comparator and temperature sensor to the integrated device structure.

8. ACKNOWLEDGEMENT

9. REFERENCES

1. S.D. Senturia, C.M. Sechen, and J.A. Wishneusky, Appl. Phys. Lett., 30, 106 (1977).

2. S.D. Senturia, N.F. Sheppard, S.Y. Poh, and H.R. Appelman, Polymer Eng. and Sci., in press. Also issued as Technical Report No. 1 in this series.

3. S.L. Garverick and S.D. Senturia, 1980 IEDM Technical Digest, paper 26.6, p. 685 (1980)

4. P. Hedvig, Dielectric Spectroscopy of Polymers, Wiley, New York, (1977).

APPENDIX: TRANSFER FUNCTION MODEL

For a voltage $V_o e^{j\omega t}$ applied to the driven gate of the model of Figure 2, the complex voltage at the sensing electrode is of the form

$$V_{FG} = \frac{V_o}{A + jB}$$

The magnitude of the sensing electrode voltage will be

$$|V_{FG}| = \frac{V_o}{\sqrt{A^2 + B^2}}$$

The phase shift relative to the driving voltage will be

$$V_{FG} = -\tan^{-1}\left(\frac{B}{A}\right)$$

where $A = \cosh(m'x_o)\cos(m''x_o)$
$\qquad + a\sinh(m'x_o)\cos(m''x_o)$
$\qquad - b\cosh(m'x_o)\sin(m''x_o)$

$\quad B = \sinh(m'x_o)\cos(m''x_o)$
$\qquad + b\sinh(m'x_o)\cos(m''x_o)$
$\qquad + a\cosh(m'x_o)\sin(m''x_o)$

and

$$a = \frac{\omega R_A C_G (m'' + \omega m' R_A C_A)}{(1+\omega^2 R_A^2 C_A^2)(m'^2 + m''^2)}$$

$$b = \frac{\omega R_A C_G (m' - \omega m'' R_A C_A)}{(1+\omega^2 R_A^2 C_A^2)(m'^2 + m''^2)}$$

$$m' = \sqrt{\frac{\omega R_A C_T}{2} \frac{(\sqrt{1+\omega^2 R_A^2 C_A^2} + \omega R_A C_A)}{(1+\omega^2 R_A^2 C_A^2)}}$$

$$m'' = \sqrt{\frac{\omega R_A C_T}{2} \frac{(\sqrt{1+\omega^2 R_A^2 C_A^2} - \omega R_A C_A)}{(1+\omega^2 R_A^2 C_A^2)}}$$

Expressed in terms of permittivity, ϵ' and loss factor, ϵ'', and a thickness parameter, d,

$$R_A = 1/\omega\epsilon''d \qquad C_A = \epsilon'd$$

The constants used in evaluating these expressions were:

C_G = capacitance parameters of sensing electrode = 7.3×10^{-15} F

C_{ox} = capacitance of insulating oxide per unit area = 6.4×10^{-9} F/cm^2

x_o = distance between driven and sensing electrodes = 12.5 microns

d = thickness parameter = 12.5 microns

TECHNICAL REPORT DISTRIBUTION LIST, GEN

	No. Copies		No. Copies
Office of Naval Research Attn: Code 472 800 North Quincy Street Arlington, Virginia 22217	2	U.S. Army Research Office Attn: CRD-AA-IP P.O. Box 1211 Research Triangle Park, N.C. 27709	1
ONR Branch Office Attn: Dr. George Sandoz 536 S. Clark Street Chicago, Illinois 60605	1	Naval Ocean Systems Center Attn: Mr. Joe McCartney San Diego, California 92152	1
ONR Area Office Attn: Scientific Dept. 715 Broadway New York, New York 10003	1	Naval Weapons Center Attn: Dr. A. B. Amster, Chemistry Division China Lake, California 93555	1
ONR Western Regional Office 1030 East Green Street Pasadena, California 91106	1	Naval Civil Engineering Laboratory Attn: Dr. R. W. Drisko Port Hueneme, California 93401	1
ONR Eastern/Central Regional Office Attn: Dr. L. H. Peebles Building 114, Section D 666 Summer Street Boston, Massachusetts 02210	1	Department of Physics & Chemistry Naval Postgraduate School Monterey, California 93940	1
Director, Naval Research Laboratory Attn: Code 6100 Washington, D.C. 20390	1	Dr. A. L. Slafkosky Scientific Advisor Commandant of the Marine Corps (Code RD-1) Washington, D.C. 20380	1
The Assistant Secretary of the Navy (RE&S) Department of the Navy Room 4E736, Pentagon Washington, D.C. 20350	1	Office of Naval Research Attn: Dr. Richard S. Miller 800 N. Quincy Street Arlington, Virginia 22217	1

Commander, Naval Air Systems Command
Attn: Code 310C (H. Rosenwasser)
Department of the Navy
Washington, D.C. 20360
	1	Naval Ship Research and Development
		  Center
		Attn: Dr. G. Bosmajian, Applied
		  Chemistry Division
		Annapolis, Maryland 21401
			1

Defense Technical Information Center Building 5, Cameron Station Alexandria, Virginia 22314	12	Naval Ocean Systems Center Attn: Dr. S. Yamamoto, Marine Sciences Division San Diego, California 91232	1
Dr. Fred Saalfeld Chemistry Division, Code 6100 Naval Research Laboratory Washington, D.C. 20375	1	Mr. John Boyle Materials Branch Naval Ship Engineering Center Philadelphia, Pennsylvania 19112	1

TECHNICAL REPORT DISTRIBUTION LIST, GEN

No.
Copies

Dr. Rudolph J. Marcus
Office of Naval Research
Scientific Liaison Group
American Embassy
APO San Francisco   96503   1

Mr. James Kelley
DTNSRDC Code 2803
Annapolis, Maryland   21402   1

Dr. Henry Wohltjen   1
Naval Research Laboratory
Code 6170
Washington, DC 20390

Dr. Ron Trabocco   1
Code 60631
Naval Air Development Center
Warminster PA 18974

SP472-3/B5

TECHNICAL REPORT DISTRIBUTION LIST, 356A

	No. Copies		No. Copies
Dr. Stephen H. Carr Department of Materials Science Northwestern University Evanston, Illinois 60201	1	Picatinny Arsenal Attn: A. M. Anzalone, Building 3401 SMUPA-FR-M-D Dover, New Jersey 07801	1
Dr. M. Broadhurst Bulk Properties Section National Bureau of Standards U.S. Department of Commerce Washington, D.C. 20234	2	Dr. J. K. Gillham Department of Chemistry Princeton University Princeton, New Jersey 08540	1
Professor G. Whitesides Department of Chemistry Massachusetts Institute of Technology Cambridge, Massachusetts 02139	1	Douglas Aircraft Co. Attn: Technical Library Cl 290/36-84 AUTO-Sutton 3855 Lakewood Boulevard Long Beach, California 90846	1
Professor J. Wang Department of Chemistry University of Utah Salt Lake City, Utah 84112	1	Dr. E. Baer Department of Macromolecular Science Case Western Reserve University Cleveland, Ohio 44106	1
Dr. V. Stannett Department of Chemical Engineering North Carolina State University Raleigh, North Carolina 27607	1	Dr. K. D. Pae Department of Mechanics and Materials Science Rutgers University New Brunswick, New Jersey 08903	1
Dr. D. R. Uhlmann Department of Metallurgy and Material Science Massachusetts Institute of Technology Cambridge, Massachusetts 02139	1	NASA-Lewis Research Center Attn: Dr. T. T. Serofini, MS-49-1 21000 Brookpark Road Cleveland, Ohio 44135	1
Naval Surface Weapons Center Attn: Dr. J. M. Augl, Dr. B. Hartman White Oak Silver Spring, Maryland 20910	1	Dr. Charles H. Sherman Code TD 121 Naval Underwater Systems Center New London, Connecticut	1
Dr. G. Goodman Globe Union Incorporated 5757 North Green Bay Avenue Milwaukee, Wisconsin 53201	1	Dr. William Risen Department of Chemistry Brown University Providence, Rhode Island 02192	1
Professor Hatsuo Ishida Department of Macromolecular Science Case-Western Reserve University Cleveland, Ohio 44106	1	Dr. Alan Gent Department of Physics University of Akron Akron, Ohio 44304	1

TECHNICAL REPORT DISTRIBUTION LIST, 356A

	No. Copies		No. Copies

Mr. Robert W. Jones
Advanced Projects Manager
Hughes Aircraft Company
Mail Station D 132
Culver City, California 90230 — 1

Dr. C. Giori
IIT Research Institute
10 West 35 Street
Chicago, Illinois 60616 — 1

Dr. M. Litt
Department of Macromolecular Science
Case Western Reserve University
Cleveland, Ohio 44106 — 1

Dr. R. S. Roe
Department of of Materials Science
   and Metallurgical Engineering
University of Cincinnati
Cincinnati, Ohio 45221 — 1

Dr. Robert E. Cohen
Chemical Engineering Department
Massachusetts Institute of Technology
Cambridge, Massachusetts 02139 — 1

Dr. T. P. Conlon, Jr., Code 3622
Sandia Laboratories
Sandia Corporation
Albuquerque, New Mexico — 1

Dr. Martin Kaufmann, Head
Materials Research Branch, Code 4542
Naval Weapons Center
China Lake, California 93555 — 1

Dr. T. J. Reinhart, Jr., Chief
Composite and Fibrous Materials Branch
Nonmetallic Materials Division
Department of the Air Force
Air Force Materials Laboratory (AFSC)
Wright-Patterson AFB, Ohio 45433 — 1

Dr. J. Lando
Department of Macromolecular Science
Case Western Reserve University
Cleveland, Ohio 44106 — 1

Dr. J. White
Chemical and Metallurgical Engineering
University of Tennessee
Knoxville, Tennessee 37916 — 1

Dr. J. A. Manson
Materials Research Center
Lehigh University
Bethlehem, Pennsylvania 18015 — 1

Dr. R. F. Helmreich
Contract RD&E
Dow Chemical Co.
Midland, Michigan 48640 — 1

Dr. R. S. Porter
Department of Polymer Science
   and Engineering
University of Massachusetts
Amherst, Massachusetts 01002 — 1

Professor Garth Wilkes
Department of Chemical Engineering
Virginia Polytechnic Institute and
   State University
Blacksburg, Virginia 24061 — 1

Dr. Kurt Baum
Fluorochem Inc.
6233 North Irwindale Avenue
Azuza, California 91702 — 1

Professor C. S. Paik Sung
Department of Materials Sciences and
   Engineering Room 8-109
Massachusetts Institute of Technology
Cambridge, Massachusetts 02139 — 1